


Article

Extracellular Polymeric Substances Protect *Chlorella* sp. Against the Cadmium Stress

Fangyuan Liu ¹, Xingye Han ¹, Zhengyang Wang ², Xuefeng Zhao ², Yibo Zhang ³ and Hongmei Ge ^{1,4,*} 

¹ Hubei Key Laboratory of Environmental Geotechnology and Ecological Remediation for Lake & River, Hubei University of Technology, Wuhan 430068, China

² Hanjiang Bureau of Hydrology and Water Resources, Bureau of Hydrology, Changjiang Water Resources Commission, Xiangyang 441000, China; xuefengzhao@sina.com (X.Z.)

³ School of Environmental Science and Engineering, Huazhong University of Science and Technology, Wuhan 430074, China

⁴ Innovation Demonstration Base of Ecological Environment Geotechnical and Ecological Restoration of Rivers and Lakes, School of Civil Engineering, Architecture and Environment, Hubei University of Technology, Wuhan 430068, China

* Correspondence: gehongmei@hbut.edu.cn

Abstract

Extracellular polymeric substances (EPS) are secreted by microalgae and contribute to protecting cells from damage induced by cadmium (Cd) exposure. However, the response mechanism of *Chlorella* sp. to Cd(II) stress as well as associated changes in the chemical properties (including functional groups and composition) of soluble EPS (SL-EPS), loosely bound EPS (LB-EPS), and tightly bound EPS (TB-EPS) in this microalga, remain unclear. This study aimed to investigate the role of EPS in enabling *Chlorella* sp. to resist Cd(II) stress. The results demonstrated that Cd(II) stress resulted in a significant inhibition of algal, chlorophyll a (Chl a) contents, and maximum photochemical quantum yield (F_v/F_m) of *Chlorella* sp., with 7 d EC₃₀ of 6 mg/L. Nevertheless, Cd(II) exposure significantly increased both superoxide dismutase (SOD) activity and EPS content. Fourier transform infrared (FTIR) spectroscopic analysis revealed that differences existed in the functional groups involved in Cd(II) binding across algal cell density, SL-EPS, LB-EPS, and TB-EPS. The carboxyl group was identified as the most prominent functional group and were found to play a crucial role in the adsorption of Cd(II). Additionally, Tryptophan-like protein substance in EPS may be the main component binding with Cd(II) in *Chlorella* sp. This study indicated that *Chlorella* sp. resisted Cd(II) stress by increasing SOD activity and EPS content, with protein-like substance containing tryptophan proteins in EPS which could also contribute to protection against Cd stress.

Keywords: *Chlorella* sp.; cadmium; EPS; FTIR



Received: 8 August 2025

Revised: 16 September 2025

Accepted: 24 September 2025

Published: 29 September 2025

Citation: Liu, F.; Han, X.; Wang, Z.; Zhao, X.; Zhang, Y.; Ge, H.

Extracellular Polymeric Substances Protect *Chlorella* sp. Against the Cadmium Stress. *Ecologies* **2025**, *6*, 65. <https://doi.org/10.3390/ecologies6040065>

Copyright: © 2025 by the authors. Licensee MDPI, Basel, Switzerland. This article is an open access article distributed under the terms and conditions of the Creative Commons Attribution (CC BY) license (<https://creativecommons.org/licenses/by/4.0/>).

1. Introduction

Cadmium (Cd) pollution has become a global challenge for environmental sustainability due to its high toxicity, bioaccumulation potential, and persistence [1]. Driven by industrial and agricultural development, Cd is continuously released into aquatic environments, posing severe threats to ecosystem stability, food safety, and ultimately human health through its accumulation in food chains. In Asia, the average concentration of Cd in surface water reaches $17.75 \pm 3.96 \mu\text{g/L}$, exceeding the World Health Organization (WHO) threshold limit of $3 \mu\text{g/L}$. Cd [2,3]. In industrial effluents, particularly electroplating

wastewater, Cd concentrations typically range from 0.03 to 102 mg/L, and in extreme cases can be as high as 1570 mg/L [4]. These findings highlight the urgent need for sustainable remediation technologies in highly contaminated regions.

Conventional remediation techniques, including adsorption, precipitation, chemical reduction, ion exchange, and evaporation, are often limited by high operational costs, secondary pollution, or inefficiency at low metal concentrations. In contrast, microalgae have been widely employed in bioremediation of heavy metals due to their high metal adsorption efficiency, environmental sustainability, and renewability [5–8]. For example, certain *Scenedesmus quadricauda* can achieve exceptionally rapid metal removal, with one study reporting a 100% removal rate of Cr(VI) within 4 h [9]. The high efficiency of microalgae is also evident in the removal of Pb, with *Chlorella* sp. achieving a 78% removal rate within 3 h [10]. These cases illustrate the remarkable potential of microalgae for rapid and effective heavy metal removal.

To mitigate the toxic effects of heavy metals, microalgae employ various strategies, such as extracellular immobilization, intracellular sequestration, and activation of antioxidant defense systems [11]. Among these, biosorption is the primary mechanism underlying extracellular immobilization, involving the binding of heavy metals to charged macromolecules on the cell surface, typically through complexation, ion exchange, surface precipitation, and redox reactions [12,13]. Due to the presence of numerous negatively charged functional groups (e.g., carboxyl, hydroxyl, amino, and sulfhydryl groups) on EPS associated with the cell wall, metal ions can be efficiently adsorbed onto the cell surface during this process [12–14]. The efficiency of this adsorption process is further modulated by several environmental and biological factors. For instance, algae generally exhibit higher adsorption efficiencies under neutral to weakly acidic conditions, whereas efficiency decreases sharply at higher pH due to metal ion precipitation in alkaline environments [14]. Moreover, adsorption capacity tends to be greater for metal ions with higher electronegativity when comparing ions of similar size. The binding ability of EPS is strongly influenced by the abundance of negatively charged groups on its surface.

At the intracellular level, heavy metals are chelated intracellularly by specific molecules such as metallothioneins (MTs), phytochelatins (PCs), and glutathione (GSH), which constitute the primary metal-binding systems in microalgae [11]. Metallothioneins are cysteine-rich proteins that bind Cd via thiol groups, while phytochelatins are enzymatically synthesized from glutathione by phytochelatin synthase (PCS) and play a central role in intracellular Cd sequestration and detoxification. Meanwhile, oxidative damage caused by heavy-metal-induced reactive oxygen species (ROS) is further mitigated by antioxidant enzymes such as superoxide dismutase, catalase, ascorbate peroxidase, and glutathione reductase. Notably, the structure and composition of EPS in different microalgae can be altered in response to various heavy metal treatments [15–17]. Therefore, the specific strategies employed by microalgae to counteract the toxicity of different heavy metals warrant further investigation.

Chlorella sp. is a green algae well-known for its high production of lipids and polysaccharides [18,19]. Studies indicate that *Chlorella* sp. mitigates heavy metal toxicity and purifies wastewater through the secretion of large quantities of EPS [20]. However, it remains unclear which specific aspects of the chemical structure of EPS are affected by Cd(II) stress, particularly regarding the role of functional groups (e.g., carboxyl, hydroxyl, amide), the relative protein–polysaccharide composition, and the differential responses among SL-EPS, LB-EPS, and TB-EPS. In this work, we aim to illustrate the role of EPS in protecting *Chlorella* sp. against Cd(II) stress by analyzing biochemical generation, compositional characteristics, and functional group profiles of different types of EPS. These findings are of great significance for the application of algae in bioremediation of heavy metal.

2. Materials and Methods

2.1. Growth Conditions of *Chlorella* sp.

Chlorella sp. FACHB-1227 was obtained from the Freshwater Algae Culture Collection of the Institute of Hydrobiology, Chinese Academy of Sciences. The algae were cultured in Erlenmeyer flasks containing sterilized BG11 medium (pH 7.1). Cultures were maintained at 25 ± 1 °C under a 12/12 h light/dark cycle with an incident light intensity of approximately $36 \mu\text{mol photons m}^{-2} \text{s}^{-1}$. Cells used for the experiments were in the logarithmic growth phase, specifically within the range of $\text{OD}_{680} = 0.2\text{--}0.5$ (corresponding to approximately $3 \times 10^6\text{--}8 \times 10^6$ cells mL^{-1}). To prevent contamination from residual metals, all glassware underwent pretreatment involving a seven-day soak in 10% hydrochloric acid and was then carefully rinsed with deionized water. Prior to use, culture flasks were covered with sterile, gas-permeable sealing films and sterilized by autoclaving. During cultivation, the flasks were periodically shaken and their positions were frequently changed for ensuring uniform light exposure and avoiding adhesion of algal cells to the flask walls.

1000 $\text{mg}\cdot\text{L}^{-1}$ Cd(II) stock solution was prepared using $\text{CdCl}_2\cdot 2.5\text{H}_2\text{O}$ and diluted with BG11 medium to generate obtain five working concentrations: 3, 6, 10, 15, and 20 mg/L , with an initial cell density about 5×10^6 cells/mL. Each treatment group and its CdCl₂-free control were prepared in three replicates. Cell growth was monitored daily by counting cell numbers using a hemocytometer. EC_{50} was determined via a chemical algal growth inhibition test following previously established methods [21].

2.2. Cd(II) Removal

Chlorella sp. cultures were treated with 6 mg/L Cd(II) in BG11 medium for a period of seven days. Cd(II) removal was assessed by separating the metal into three fractions: residual Cd(II) remaining in the medium, Cd(II) bound to EPS on the cell surface, and Cd(II) accumulated within the cells. The extraction procedures followed the method described by Ozturk et al. [21]. After centrifugation at $10,000\times g$, the supernatant was analyzed to quantify the residual Cd(II) in the medium. On the 7th day, the resulting pellets were treated with 10 mmol/L EDTA to desorb Cd(II) from the cell surface and centrifuged again at $10,000\times g$. The supernatant obtained at this step was examined for EPS-associated Cd(II). The remaining pellets were digested with nitric and perchloric acids to determine intracellular Cd(II). Final Cd(II) concentrations were quantified using an atomic absorption spectrophotometer (AA-6880, Shimadzu Corporation, Shimadzu, Kyoto, Japan).

$$\text{Cd(II)removal efficiency (\%)} = \frac{\text{Initial Cd(II)amount} - \text{Residual Cd(II)amount in BG11}}{\text{Initial Cd(II)amount}}$$

2.3. Determination of Chl *a* and Maximal Chlorophyll Fluorescence of PSII (*Fv* /*Fm*)

Pigments analysis of algal samples was carried out according to the procedure of Sartory and Grobbelaar [22]. The algal samples were first centrifuged at $5000\times g$ for 15 min. The resulting pellet was then extracted with 95% ethanol for 24 h in the dark at 4 °C. After a final centrifugation of the extract at $4000\times g$ for 10 min, the resulting supernatant was collected for subsequent analysis. The Chl *a* concentration was then quantified by recording absorbance at 665 and 649 nm.

Meanwhile, 5 mL of *Chlorella* sp. suspensions were dark-adapted for 10 min, and *Fv* /*Fm* was measured using a water sample chlorophyll fluorometer (WALZ, PAM-2500, Effeltrich, Germany) with a saturating light intensity of $1500 \mu\text{E}\cdot\text{m}^{-2} \text{s}^{-1}$.

2.4. Measurement of Malondialdehyde (MDA) and Superoxide Dismutase (SOD) Content

Algal cells exposed to 6 mg/L Cd(II) or maintained without Cd(II) were sampled at 0.5 h, 4 h, 24 h, 72 h, and 168 h. The algal suspensions were centrifuged at $3000\times g$ for 10 min at 4 °C to obtain cell pellets. The harvested cells were then resuspended in PBS buffer and disrupted using a tissue homogenizer under the following conditions: 45 Hz, with 30 s of grinding followed by 10 s of rest, repeated for three cycles. The homogenized mixtures were subsequently centrifuged at $2000\times g$ for 5 min at 4 °C. The resulting supernatant was used to determine the activities of MDA content and SOD activity, using corresponding commercial assay kits (Nanjing Jiancheng Bioengineering Institute, www.njjcbio.com (accessed on 15 September 2025)). Measurements were strictly performed in accordance with the manufacturer's protocol.

2.5. EPS Extraction and Determination

The algal EPS was separated into three distinct fractions: SL-EPS, LB-EPS, and TB-EPS [23,24]. Extraction of SL-EPS, LB-EPS, and TB-EPS was performed following previously described methods [24,25]. First, samples were centrifuged at $2500\times g$ for 15 min, and the supernatant was collected to analyze SL-EPS. Next, the algal pellets obtained in the previous step were suspended in 0.05% NaCl solution with a volume equal to that of the original sample, and then centrifuged at $5000\times g$ for 15 min. After collecting the supernatant for LB-EPS analysis, the pellets were resuspended in 0.05% NaCl, heated at 60 °C for 30 min, and centrifuged to obtain the TB-EPS fraction. Filtration of all EPS fractions through 0.45 µm PTFE membranes was performed to remove intact cells and large debris, ensuring that only extracellular polymers were collected and analyzed. Polysaccharide and protein contents in the EPS samples were quantified via the phenol-sulfuric acid method [26] and the Bradford method [27], respectively.

2.6. Fourier Transform Infrared Spectroscopy (FTIR) Analysis

FTIR spectroscopy was used to analyze functional groups in organic matter. On 7th day, algal cultures were centrifuged at $5000\times g$ for 15 min to collect algal biomass for further analysis. EPS fractions were subsequently isolated following the procedure outlined in Section 2.5 and dialyzed according to the method of Ge et al. [28]. Both the EPS-containing supernatants and algal pellets were lyophilized using a vacuum freeze dryer (FD-1A-50, Bio-Equip, Shanghai, China). The dried materials were then subjected to characterization by FTIR spectroscopy. (FTIR5700, Thermo Fisher Scientific, Waltham, MA, USA). Prior to FTIR analysis, all EPS subjected to identical preparation procedures, including lyophilization, fine grinding, and dialysis to remove salts and small molecules. To minimize spectral variation, the same instrumental parameters were used for all measurements (ATR mode, 4 cm^{-1} resolution, 32 scans per spectrum), and baseline correction and normalization were applied to each spectrum. Additionally, blank controls were measured to eliminate background interference.

2.7. Measurement of Three-Dimensional Fluorescence Excitation–Emission Matrix (3D-EEM)

3D-EEM was used to analyze compositional changes in organic matter including EPS. Due to the low EPS concentration after 7 days of culture, specific EPS components were not detectable by 3D-EEM; thus, the culture duration was extended to 14 days. On the 14th day, each type of EPS extracted using the method described in Section 2.5 was analyzed by a 3D-EEM (Lumina, Thermo Fisher Scientific, Waltham, MA, USA). This work adopted the specific parameters reported by Xu et al. [24].

2.8. Statistical Analysis

All experiments and analyses were conducted based on three independent biological replicates. Statistical analyses were performed with SPSS software (Version 22.0) via one-way analysis of variance (ANOVA) and Student's *t*-test. Standard errors were calculated and displayed as error bars in figures. Differences were considered statistically significant at $p < 0.05$.

3. Results and Discussion

3.1. Growth Inhibition and Cd(II) Removal by *Chlorella* sp.

The effects of different Cd(II) concentrations on the growth of *Chlorella* sp. are shown in Figure 1a. The cell density decreased significantly with increasing Cd(II) concentration ($p < 0.05$). Based on the growth inhibition results, the 2, 3, 4, and 7d EC₅₀ were calculated to be 3.873, 5.874, 7.126, and 9.547 mg/L, respectively. When the Cd(II) concentration increased from 6 mg/L to 10 mg/L, a significant decrease in biomass was observed. Based on growth inhibition data, an EC₃₀ of 6 mg/L over 7 days was selected for subsequent experiments. The inhibitory effects of Cd(II) on microalgal growth have been reported in previous studies [29,30]. The decrease in growth observed at higher Cd(II) concentrations in our study may be attributed to Cd(II)-induced damage to photosynthetic activity and the triggering of oxidative stress [29,30].

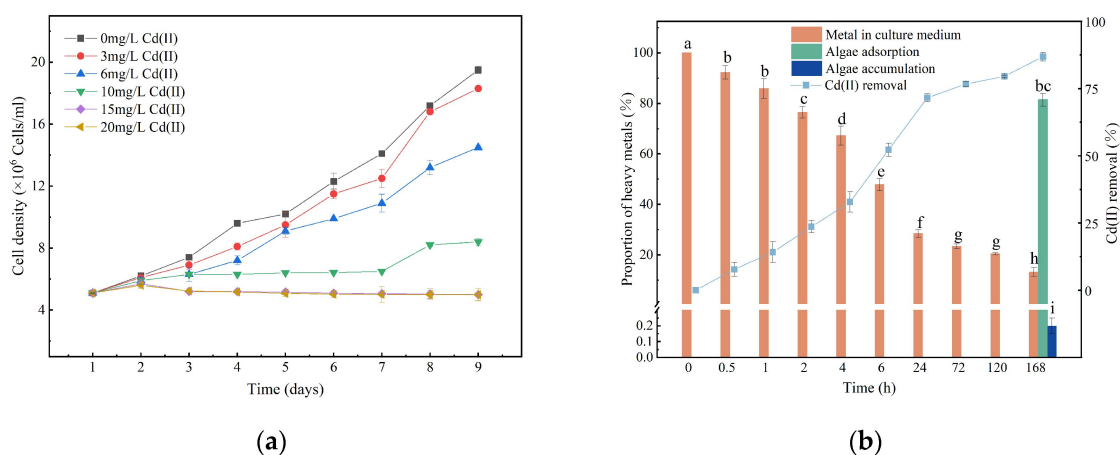


Figure 1. Growth curve (a), and Cd(II) removal efficiency when *Chlorella* sp. was exposed to 6 mg/L Cd(II) (b). Data are presented as mean \pm SD ($n = 3$). Columns sharing the same letter are not significantly different ($p > 0.05$); columns with different letters indicate significant differences ($p < 0.05$); the same applies below.

Biosorption is characterized by faster kinetics compared to bioaccumulation, which requires the activation of intracellular metal transport systems [31]. Figure 1b shows the removal efficiency of Cd(II) by *Chlorella* sp. at a concentration of 6 mg/L Cd(II). Within the first 24 h, the adsorption of Cd(II) was a rapid process and Cd(II) removal efficiency was 71.6%. The removal efficiency of Cd(II) increased gradually within 24 h, reaching 71.6%, after which the rate of increase slowed. By the conclusion of the 7th day, 13.2% of Cd(II) remained in the culture medium, while 86.8% was adsorbed by the cells. Concurrently, the proportions of Cd(II) remaining in the medium, adsorbed onto the cell surface EPS, and accumulated within the cells were determined to be 13.2%, 82.6%, and 3.8%, respectively. The fast binding of Cd(II) within 24 h implies that metal removal occurs primarily through interactions with surface functional groups [32,33]. Heavy ions can be effectively adsorbed by the cell surface, a finding consistent with previous studies [16,17]. This suggests that B-EPS plays a major role in the Cd(II) adsorption. Cd(II) adsorption is a rapid process,

probably because Cd(II) mainly interacts with acidic sites on the cell wall, such as uronic acid and carboxyl groups [32,33].

The concentration of Cd(II) in natural water systems is typically below 1 µg/L [34], and the presence of Cd(II) in municipal and typical electroplating wastewaters is typically less than 2 mg/L [16]. As illustrated in Figure 1a, exposure to 3 mg/L Cd(II) resulted in growth of *Chlorella* sp. comparable to that of the control group, indicating that *Chlorella* sp. may not suffer significant harm from Cd(II) in actual wastewater. The removal efficiency of Cd(II) was 71.6% within 24 h, indicating that *Chlorella* sp. may also serve as a promising candidate for removing Cd(II) from wastewater [5,16].

3.2. Change in Chl *a* Content and Photosynthetic Activity

The Chl *a* content in the Cd(II)-treated group decreased with prolonged cultivation time (Figure 2a). This observation is consistent with previous studies. The suppression of Chl *a* content by Cd(II) is attributed to a decline in chlorophyllides, which act as essential precursors for the synthesis of these photosynthetic pigments [35]. Additionally, the reduction in chlorophyll levels caused by Cd may be linked to oxidative stress and thylakoid lipid peroxidation, events that can cause subsequent chlorophyll degradation [36,37].

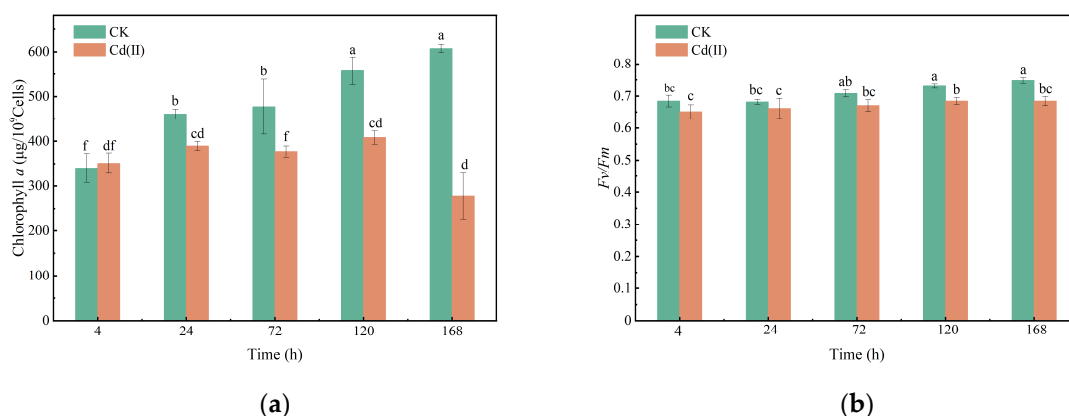


Figure 2. Changes in Chl *a* (a) and Fv/Fm (b) of *Chlorella* sp. with or without Cd(II) exposed. (“CK” refers to the control group and “Cd(II)” refers to the treatment group exposed to 6 mg/L Cd(II). The same definition applies to all figures in this manuscript.

During the initial stage of Cd(II) stress (0–24 h), Fv/Fm showed no statistically significant difference from the control group ($p > 0.05$) (Figure 2b). However, a progressive decline in Fv/Fm was observed in the Cd(II)-treated group after 120 h. Fv/Fm in *Chlorella* sp. was reduced by 6.33%, and 8.51% at 120 and 168 h of Cd(II) exposure, respectively. The inhibitory effect of Cd(II) on photosynthesis could be due to the competition of Cd(II) with calcium, magnesium, manganese, and iron ions in the photosynthetic apparatus, thereby damaging the photosynthetic electron transport chain [31,38–40]. On the other hand, Cd(II) may damage the photosystems by regulating the genes involved in chlorophyll and light-harvesting antenna protein synthesis, resulting in decreased Chl *a* contents and photosynthetic activity [40].

3.3. Change in the MDA Content and SOD Activity

MDA serves as a key indicator of oxidative damage, reflecting the extent of lipid peroxidation induced by environmental stress [35]. Significant increases in MDA content at 4 h (by 24.5%) and 24 h (by 27.9%) were observed in the 6 mg/L Cd(II) group compared with the control group (Figure 3a). It has been established in many former studies that heavy metals can induce oxidative stress [17,35]. In this work, the increased MDA content can be attributed to Cd(II)-induced oxidative stress, which triggers the accumulation of

ROS, causing lipid peroxidation and membrane damage [41,42]. However, MDA levels exhibited no significant difference from the control group as exposure time prolonged ($p > 0.05$). This finding demonstrates the metabolic adaptability of *Chlorella* sp., which can alleviate lipid peroxidation by enhancing its intrinsic antioxidant mechanisms [43].

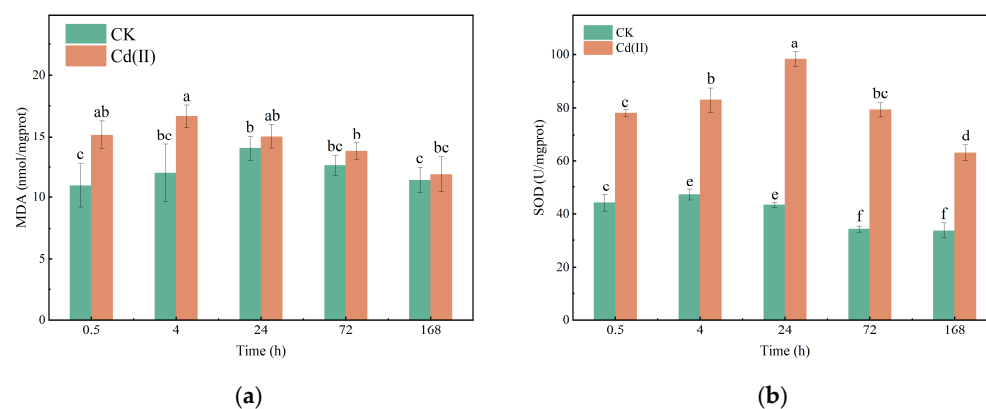


Figure 3. Changes in MDA content (a) and SOD activity (b) of *Chlorella* sp. with or without Cd(II) exposed.

SOD is a key enzyme involved in ROS scavenging and regulating cellular redox homeostasis. Cd(II) significantly increased the SOD activity by 43.6%, 43.2%, 56.0%, 56.6% and 46.4% at 4 h, 24 h, 72 h, 120 h and 168 h, respectively, compared with the control group (Figure 3b). Elevated SOD activity in response to heavy metal exposure has been documented in various algal species, including *Desmodesmus armatus* [35] and *Microcystis aeruginosa* [14]. This phenomenon indicates the activation of a rapid antioxidant response to scavenge ROS generated by heavy ions and prevent oxidative damage [44].

3.4. The Role of EPS in Metal Sequestration

3.4.1. Changes in Polysaccharides and Proteins Contents in EPS

As shown in Figure 4, the polysaccharides contents in EPS was higher than proteins in both Cd(II)-exposed and unexposed conditions ($p < 0.05$). Cd(II) stress led to an accumulation of polysaccharides and proteins within the SL-EPS and B-EPS fractions. The maximum polysaccharides and proteins contents in EPS reached 4.18 and 0.686 pg/cell, respectively. This provides further support for the hypothesis that Cd(II) can induce EPS production [16,17]. EPS secretion is considered as a defensive mechanism by *Microcystis aeruginosa* [17] and *Spirulina platensis* [16] under Cd(II) stress, suggesting that *Chlorella* sp. may also secrete EPS to defend against the Cd(II) stress in the present study.

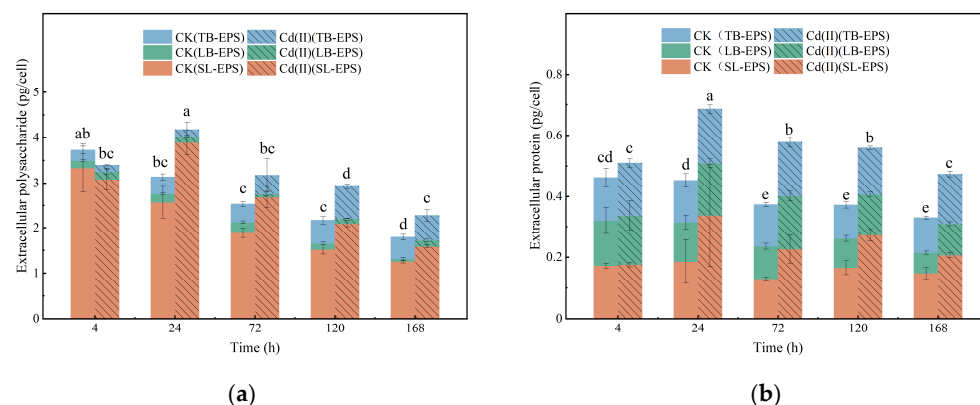


Figure 4. Variations in the content of polysaccharides (a) and proteins (b) within the EPS of *Chlorella* sp. with or without Cd(II) exposed.

3.4.2. FTIR Analysis

FTIR can be used to reveal the differences in functional groups of biological materials, thereby providing further confirmation of the binding mechanism between EPS and heavy metals. FTIR spectra of algal cells and various EPS fractions (SL-EPS, LB-EPS, TB-EPS) from *Chlorella* sp. treated with or without 6 mg/L Cd(II) are shown in Figure 5. The functional groups responsible for the biosorption of Cd(II) by the algal cells or each EPS fraction were analyzed by FTIR spectroscopy, and these groups are listed in Table 1. Characteristic peaks were observed to shift before and after metal adsorption, suggesting the adsorption sites were occupied by metal ions [45].

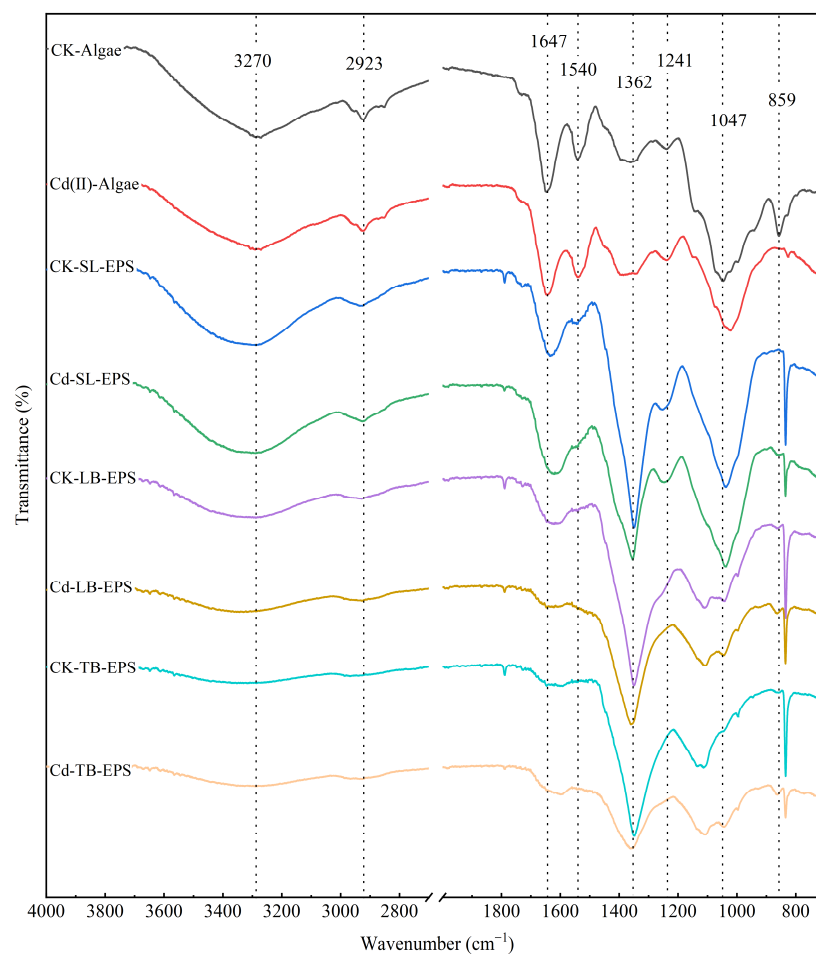


Figure 5. FTIR spectra of cellular biomass and EPS from *Chlorella* sp. treated with 0 and 6 mg/L Cd(II) exposure.

The absorption bands at 3270–3344 cm^{-1} are attributed to the stretching vibrations of $-\text{NH}_2$ or $-\text{OH}$ groups [21,46]. The strong absorption peak at 2920–2990 cm^{-1} can be assigned to stretching vibrations of unsaturated methyl group ($-\text{CH}_3$) or a hydroxyl group ($-\text{OH}$) on benzene ring [47,48]. The broad bands at 1622–1647 cm^{-1} correspond to the stretching vibrations of quinone, amide, or ketone $\text{C}=\text{O}$ bonds [49]. The peak near 1596 cm^{-1} corresponds $\text{C}=\text{C}$ stretching of aromatic and the COO^- stretching of deprotonated carboxylic acid [49]. The peak at 1360 cm^{-1} corresponds to the bending vibration of $-\text{OH}$ groups in the carboxyl group [46]. The broad bands at 1240–1255 cm^{-1} correspond to the stretching vibration of $\text{P}=\text{O}$ [14], which is a functional group present in nucleic acids, phospholipids and phosphoprotein, etc. The broad bands around 1047 cm^{-1} represent the stretching vibration $\text{C}-\text{O}-\text{C}$ linkages in polysaccharides, which can be found

in the dextran functional groups on algal cell walls [48]. The FTIR peak at 859 cm^{-1} is commonly attributed to the C–H deformation vibrations of α -pyranose rings [20].

In this study, Cd(II) exposure led to pronounced modifications in the FTIR spectra for algal cells and each type of EPS. Han et al. [17] also reported similar results in Cd(II)-treated *Microcystis aeruginosa*. Moreover, differences in major peaks among the various EPS fractions indicated that the functional groups involved in Cd(II) binding differed slightly between algal cells, SL-EPS, LB-EPS, and TB-EPS. Thus, each type of EPS plays a distinct role in adsorbing Cd(II). There were significant shift in peaks at around 1647 cm^{-1} and 1360 cm^{-1} in algal cells, SL-EPS, LB-EPS and TB-EPS (only at 1360 cm^{-1}), which correspond to C=O bond and –OH bond in the carboxyl group, respectively, before and after Cd(II) adsorption. Carboxyl groups are the most common functional groups containing a C=O bond that is negatively charged and abundant in algal cell walls [50]. These results indicated that the carboxyl group served as the key functional group in the EPS, playing a primary role in Cd(II) adsorption.

Table 1. FTIR peak wavenumber shifts in *Chlorella* sp. biomass and its EPS fractions before and after Cd(II) adsorption.

Wavenumber (cm ^{−1})									
Algae		SL-EPS		LB-EPS		TB-EPS		Functional Group	References
CK	Cd	CK	Cd	CK	Cd	CK	Cd		
-	-	3290	3304	3288	3344	3318	3287	Amino group (−NH ₂)	[46]
2923	2926	2934	2928	2932	2930	2987	2931	Methyl group (−CH ₃) or Hydroxyl group attached to aromatic rings (X−OH)	[47,48]
1647	1645	1633	1622	1622	1646			Quinone, amide, or ketone C=O bond stretching	[51]
-	-					1594	1601	C=C and the COO [−] stretching	[49]
1362	1386	1350	1354	1350	1360	1350	1362	Bending−OH (−COOH)	[46]
-	-	1255	1249					Phosphate group (P=O stretching vibration)	[14]
				1111	1108	-	-	Ether (C−O−C) in polysaccharides	[52]
1047	1023	-	-					The elongation of bonds C−C and C−O in polysaccharides	[53]
859	833	-	-	-	-	-	-	furanose and pyranose rings of saccharides α-glycosidic bonds	[20]

–: no significant shift peak point.

3.4.3. 3D-EEM Analysis

As shown in Figure 6 and Table 2, the 3D-EEM contours of the EPS contained two peaks. Peak A ($\text{Ex}/\text{Em} = 280/325\text{ nm}$) and Peak B ($\text{Ex}/\text{Em} = 365/440\text{ nm}$) were attributed to tryptophan-like protein substance and humus-like substances originating from the decomposition of macromolecular organics [54,55]. The results indicate that tryptophan-like protein substance and humus-like substances were identified in the EPS under both CdCl_2 exposure conditions (0 and 6 mg/L). The organic composition of the different EPS fractions was remarkably similar between the control and 6 mg/L Cd(II)-exposed groups (Figure 6), indicating that Cd(II) did not alter their organic composition.

SL-EPS exhibited two distinct fluorescence peaks (Peak A and Peak B), whereas LB-EPS and TB-EPS showed only Peak A (Figure 6). These findings indicate that tryptophan-containing substances are a shared component of the EPS in *Chlorella* sp., present consistently across all its EPS fractions. For the SL-EPS, due to its direct exposure to the external environment, it tends to accumulate a greater amount of soluble organics secreted through metabolism (e.g., humic-like substances). This accumulation, in turn, enables *Chlorella* sp. to respond effectively to external environmental stimuli. The treatment group showed no marked changes in EPS fluorescence regions compared to the control, whereas the fluorescence intensity of SL-EPS was significantly reduced. This finding aligns with previous studies, which have demonstrated that CdCl_2 and light intensity do not alter the

EEM contour patterns of algal EPS, but the fluorescence intensity of peaks varies across different EPS fractions depending on the treatment [15,17,56]. Specifically, Wang et al. [15] reported that 20 mg/L CdCl₂ did not modify the organic composition of EPS from *Spirulina platensis*; however, the fluorescence intensities of peaks in EPS were significantly lower in the 20 mg/L CdCl₂ treatment group than in the control group. Notably, the carboxyl (—COOH) and amino (—NH₂) groups of tryptophan are recognized as key coordination sites for heavy metals. In the present study, Cd(II) exposure reduced the fluorescence intensity of Peak A in SL-EPS relative to the control. This observation suggests that tryptophan in EPS forms highly stable complexes with heavy metal ions via functional groups including carboxyl and amino groups, leading to fluorescence quenching. Such complexation effectively reduces the toxicity of free heavy metals and prevents their entry into algal cells [14]. Collectively, these results support the inference that tryptophan-containing protein-like substances are the primary components involved in Cd(II) binding in *Chlorella* sp.

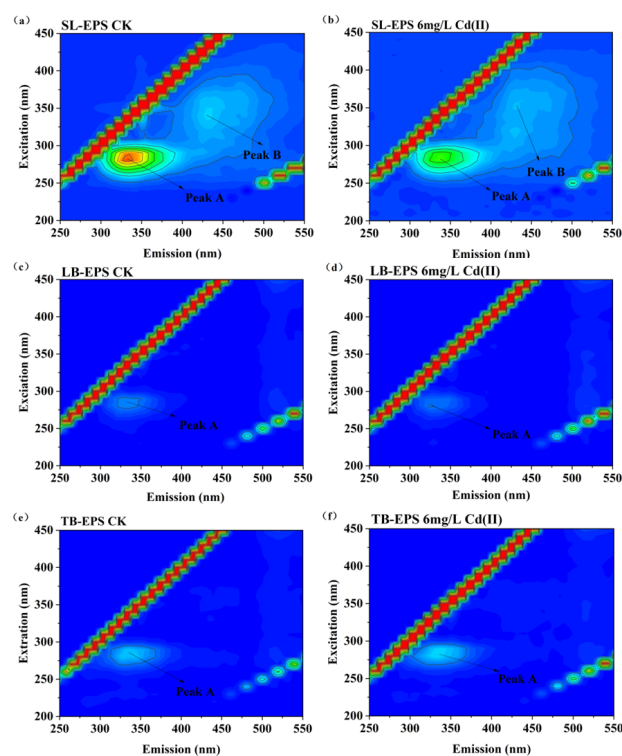


Figure 6. 3D-EEM contour plots of EPS fractions from *Chlorella* sp. with and without 6 mg/L Cd(II). Peaks A (Ex/Em 280/325 nm) and B (Ex/Em 365/440 nm) are indicated. (a) SL-EPS control (CK); (b) SL-EPS under Cd(II) treatment; (c) LB-EPS control (CK); (d) LB-EPS under Cd(II) treatment; (e) TB-EPS control (CK); (f) TB-EPS under Cd(II) treatment.

Table 2. Fluorescence spectral parameters of EPS fractions obtained from *Chlorella* sp. under Cd(II) exposure and Cd(II)-free conditions.

		Peak A (Tryptophan-Like Protein Substance)		Peak B (Humic-Like Substance)	
		Intensity	Site (Ex/Em)	Intensity	Site (Ex/Em)
SL-EPS	CK	9309.2	280/325 nm	1727.6	365/440 nm
	Cd(II)	5326.5	280/325 nm	1401.2	365/440 nm
LB-EPS	CK	1426	280/325 nm	-	-
	Cd(II)	1223.8	280/325 nm	-	-
TB-EPS	CK	2323.4	280/325 nm	-	-
	Cd(II)	2189.6	280/325 nm	-	-

-: no corresponding value or site.

3.5. Correlation Analysis

Correlation analysis was utilized to assess the associations between critical physiological responses in *Chlorella* sp. under Cd(II) stress. As shown in Figure 7, biomass exhibited a significant negative correlation with MDA levels ($p < 0.05$), suggesting that oxidative stress and lipid peroxidation directly contributed to growth inhibition. In contrast, biomass exhibited a significant positive correlation with F_v/F_m ($p < 0.05$), indicating that the maintenance of photosynthetic efficiency was essential for sustaining algal growth under Cd stress [29,30]. Moreover, biomass exhibited a significant negative correlation with the polysaccharide contents of EPS, suggesting that Cd(II) stress induced *Chlorella* sp. to allocate more photosynthetic products and metabolic energy toward the synthesis of EPS and antioxidant defenses. This reallocation likely diverted resources away from cell division and growth, thereby inhibiting biomass accumulation.

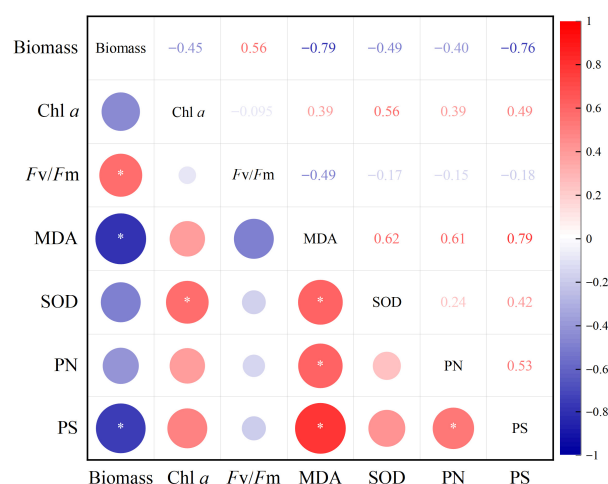


Figure 7. Correlation of indicators of *Chlorella* sp. treated with 6 mg/L Cd(II). PN and PS represents proteins and polysaccharides in the EPS, respectively.

Additionally, F_v/F_m showed a negative correlation with MDA, confirming that oxidative damage impaired photosynthetic efficiency. The positive correlations observed between MDA levels and both protein (PN) and polysaccharide (PS) contents in EPS ($p < 0.05$) highlight that oxidative stress acts as a major trigger for EPS secretion. This suggests that Cd(II)-induced lipid peroxidation [57] not only damages cellular components but also stimulates EPS production as a protective mechanism to immobilize heavy metals and alleviate toxicity [16,17]. This may represent a self-protective response by *Chlorella* sp. to resist Cd(II) toxicity.

4. Conclusions

This work systematically examined the adaptive response of *Chlorella* sp. to Cd(II) stress. The final Cd(II) adsorption efficiency reached 86.8% when the Cd(II) concentration was 6 mg/L. Cd(II) stress significantly decreased biomass, chlorophyll content, and F_v/F_m values. Moreover, EPS played a crucial role in protecting *Chlorella* sp. against Cd(II) toxicity. Under Cd(II) exposure, EPS secretion increased markedly, and functional groups such as hydroxyl, carboxyl, and amide groups, together with tryptophan-containing protein-like substances, actively participated in Cd(II) binding, thereby mitigating cellular damage. These findings supply preliminary evidence for the potential application of EPS in heavy metal bioremediation.

Nevertheless, limitations of this study should be acknowledged. The experiments were conducted under controlled laboratory conditions with Cd(II) concentrations exceeding those typically observed in natural waters. Furthermore, EPS characterization was limited

to FTIR and 3D-EEM analyses. Future studies should be conducted under more realistic environmental conditions to further validate the protective function of EPS in *Chlorella* sp. against Cd(II) stress.

Author Contributions: F.L.: Writing—original draft, Methodology, Investigation, Formal analysis; X.H.: Writing—review and editing, data curation. Methodology; Z.W.: Writing—review and editing; X.Z.: Writing—review and editing; Y.Z.: Writing—review and editing; H.G.: Conceptualization, Supervision, Writing—review and editing, Funding acquisition. All authors have read and agreed to the published version of the manuscript.

Funding: This study was supported by the National Natural Science Foundation of China (Nos. 31800457) and Open Project Funding of Hubei Key Laboratory of Environmental Geotechnology and Ecological Remediation for Lake & River, Hubei University of Technology (HJKFYP202502).

Data Availability Statement: Data contained in the study are available from the authors upon reasonable request.

Conflicts of Interest: The authors declare no conflicts of interest.

Abbreviations

The following abbreviations are used in this manuscript:

Cd	Cadmium
ROS	Oxygen species
EPS	extracellular polymeric substances
SL-EPS	soluble EPS
LB-EPS	Loosely bound EPS
TB- EPS	Tightly bound EPS
Chl <i>a</i>	Chlorophyll <i>a</i>
<i>F_v/F_m</i>	Maximum photochemical quantum yield
SOD	Superoxide dismutase
FTIR	Fourier transform infrared spectrum
MDA	Malondialdehyde
3D-EEM	Three-dimensional fluorescence excitation–emission matrix
PS	Polysaccharide
PN	Protein
CK	Control group

References

1. Raza, A.; Habib, M.; Kakavand, S.N.; Zahid, Z.; Zahra, N.; Sharif, R.; Hasanuzzaman, M. Phytoremediation of Cadmium: Physiological, Biochemical, and Molecular Mechanisms. *Biology* **2020**, *9*, 177. [\[CrossRef\]](#)
2. World Health Organization. *Guidelines for Drinking-Water Quality*; World Health Organization: Geneva, Switzerland, 2011; Volume 38, pp. 104–108.
3. Wu, Y.Y.; Tian, W.F.; Cheng, C.X.; Yang, L.; Ye, Q.Q.; Li, W.H.; Jiang, J.Y. Effects of cadmium exposure on metabolism, antioxidant defense, immune function, and the hepatopancreas transcriptome of *Cipangopaludina cathayensis*. *Ecotoxicol. Environ. Saf.* **2023**, *264*, 115416. [\[CrossRef\]](#)
4. Eniola, J.O.; Sizirici, B.; Stephen, S.; Yildiz, I.; Khaleel, A.; El Fadel, M. A new synthesis route of hydrothermally carbonized Na₂CO₃ activated bentonite-clay as a novel adsorbent for cadmium removal from wastewater. *Sep. Purif. Technol.* **2024**, *350*, 127960. [\[CrossRef\]](#)
5. Yan, C.; Qu, Z.; Wang, J.; Cao, L.; Han, Q. Microalgal bioremediation of heavy metal pollution in water: Recent advances, challenges, and prospects. *Chemosphere* **2022**, *286*, 131870. [\[CrossRef\]](#) [\[PubMed\]](#)
6. Sun, X.; Huang, H.; Zhu, Y.; Du, Y.; Yao, L.; Jiang, X.; Gao, P. Adsorption of Pb²⁺ and Cd²⁺ onto *Spirulina platensis* harvested by polyacrylamide in single and binary solution systems. *Colloids Surf. A Physicochem. Eng. Asp.* **2019**, *583*, 123926. [\[CrossRef\]](#)
7. Ravikumar, Y.; Razack, S.A.; Yun, J.; Zhang, G.; Zabel, H.M.; Qi, X. Recent advances in Microalgae-based distillery wastewater treatment. *Environ. Technol. Innov.* **2021**, *24*, 101839. [\[CrossRef\]](#)

8. Gondi, R.; Kavitha, S.; Kannah, R.Y.; Karthikeyan, O.P.; Kumar, G.; Tyagi, V.K.; Banu, J.R. Algal-based system for removal of emerging pollutants from wastewater: A review. *Bioresour. Technol.* **2022**, *344*, 126245. [\[CrossRef\]](#)
9. Daneshvar, E.; Zarrinmehr, M.J.; Kousha, M.; Hashtjin, A.M.; Saratale, G.D.; Maiti, A.; Vithanage, M.; Bhatnagar, A. Hexavalent chromium removal from water by microalgal-based materials: Adsorption, desorption and recovery studies. *Bioresour. Technol.* **2019**, *293*, 122064. [\[CrossRef\]](#)
10. Molazadeh, P.; Khanjani, N.; Rahimi, M.; Nasiri, A. Adsorption of Lead by Microalgae *Chaetoceros* Sp. and *Chlorella* Sp. from Aqueous Solution. *J. Community Health Res.* **2015**, *4*, 114–127.
11. Zhu, Q.; Zhang, M.; Bao, J.; Liu, J. Physiological, metabolomic, and transcriptomic analyses reveal the dynamic redox homeostasis upon extended exposure of *Dunaliella salina* GY-H13 cells to Cd. *Ecotoxicol. Environ. Saf.* **2021**, *223*, 112593. [\[CrossRef\]](#)
12. Wei, L.; Li, J.; Xue, M.; Wang, S.; Li, Q.; Qin, K.; Jiang, J.; Ding, J.; Zhao, Q. Adsorption behaviors of Cu²⁺, Zn²⁺ and Cd²⁺ onto proteins, humic acid, and polysaccharides extracted from sludge EPS: Sorption properties and mechanisms. *Bioresour. Technol.* **2019**, *291*, 121868. [\[CrossRef\]](#)
13. Li, M.; Ma, C.; Yin, X.; Zhang, L.; Tian, X.; Chen, Q.; Wang, L. Investigating trivalent chromium biosorption-driven extracellular polymeric substances changes of *Synechocystis* sp. PCC 7806 by parallel factor analysis (PARAFAC) analysis. *Bioresour. Technol. Rep.* **2019**, *7*, 100249. [\[CrossRef\]](#)
14. Gu, S.; Lan, C.Q. Biosorption of heavy metal ions by green alga *Neochloris oleoabundans*: Effects of metal ion properties and cell wall structure. *J. Hazard. Mater.* **2021**, *418*, 126336. [\[CrossRef\]](#) [\[PubMed\]](#)
15. Wang, X.; Li, Y.; Zhang, X.; Chen, X.; Wang, X.; Yu, D.; Ge, B. The extracellular polymeric substances (EPS) accumulation of *Spirulina platensis* responding to Cadmium (Cd²⁺) exposure. *J. Hazard. Mater.* **2024**, *470*, 134244. [\[CrossRef\]](#) [\[PubMed\]](#)
16. Wang, J.; Tian, Q.; Zhou, H.; Kang, J.; Yu, X.; Qiu, G.; Shen, L. Physiological regulation of microalgae under cadmium stress and response mechanisms of time-series analysis using metabolomics. *Sci. Total Environ.* **2024**, *916*, 170278. [\[CrossRef\]](#)
17. Han, X.; Liu, F.; Zhang, Y.; Cheng, K.; Wang, H.; Ge, H. Detoxification strategy of *Microcystis aeruginosa* to the toxicity of Cd (II): Role of EPS in alleviating toxicity. *J. Oceanol. Limnol.* **2024**, *42*, 802–815. [\[CrossRef\]](#)
18. Mendes, A.R.; Spínola, M.P.; Lordelo, M.; Prates, J.A. Chemical compounds, bioactivities, and applications of *Chlorella vulgaris* in food, feed and medicine. *Appl. Sci.* **2024**, *14*, 10810. [\[CrossRef\]](#)
19. Sathasivam, R.; Radhakrishnan, R.; Hashem, A.; Abd_Allah, E.F. Microalgae metabolites: A rich source for food and medicine. *Saudi J. Biol. Sci.* **2019**, *26*, 709–722. [\[CrossRef\]](#)
20. Ciempiel, W.; Czemierska, M.; Szymańska-Chargot, M.; Zdunek, A.; Wiącek, D.; Jarosz-Wilkolazka, A.; Krzemińska, I. Soluble Extracellular Polymeric Substances Produced by *Parachlorella kessleri* and *Chlorella vulgaris*: Biochemical Characterization and Assessment of Their Cadmium and Lead Sorption Abilities. *Molecules* **2022**, *27*, 7153. [\[CrossRef\]](#)
21. Ozturk, S.; Aslim, B.; Suludere, Z.; Tan, S. Metal removal of cyanobacterial exopolysaccharides by uronic acid content and monosaccharide composition. *Carbohydr. Polym.* **2014**, *101*, 265–271. [\[CrossRef\]](#)
22. Sartory, D.P.; Grobbelaar, J.U. Extraction of chlorophyll a from freshwater phytoplankton for spectrophotometric analysis. *Hydrobiologia* **1984**, *114*, 177–187. [\[CrossRef\]](#)
23. Sheng, G.-P.; Yu, H.-Q.; Li, X.-Y. Extracellular polymeric substances (EPS) of microbial aggregates in biological wastewater treatment systems: A review. *Biotechnol. Adv.* **2010**, *28*, 882–894. [\[CrossRef\]](#) [\[PubMed\]](#)
24. Xu, H.; Cai, H.; Yu, G.; Jiang, H. Insights into extracellular polymeric substances of cyanobacterium *Microcystis aeruginosa* using fractionation procedure and parallel factor analysis. *Water Res.* **2013**, *47*, 2005–2014. [\[CrossRef\]](#) [\[PubMed\]](#)
25. Christenson, L.; Sims, R. Production and harvesting of microalgae for wastewater treatment, biofuels, and bioproducts. *Biotechnol. Adv.* **2011**, *29*, 686–702. [\[CrossRef\]](#) [\[PubMed\]](#)
26. DuBois, M.; Gilles, K.A.; Hamilton, J.K.; Rebers, P.A.; Smith, F. Colorimetric Method for Determination of Sugars and Related Substances. *Anal. Chem.* **1956**, *28*, 350–356. [\[CrossRef\]](#)
27. Bradford, M.M. A rapid and sensitive method for the quantitation of microgram quantities of protein utilizing the principle of protein-dye binding. *Anal. Biochem.* **1976**, *72*, 248–254. [\[CrossRef\]](#)
28. Ge, H.; Zhang, J.; Zhou, X.; Xia, L.; Hu, C. Effects of light intensity on components and topographical structures of extracellular polymeric substances from *Microcoleus vaginatus* (Cyanophyceae). *Phycologia* **2014**, *53*, 167–173. [\[CrossRef\]](#)
29. Ran, Y.; Sun, D.; Liu, X.; Zhang, L.; Niu, Z.; Chai, T.; Hu, Z.; Qiao, K. *Chlorella pyrenoidosa* as a potential bioremediator: Its tolerance and molecular responses to cadmium and lead. *Sci. Total Environ.* **2024**, *912*, 168712. [\[CrossRef\]](#)
30. Shin, J.; Kim, H.-S.; Bui, Q.T.N.; Kim, T.; Ki, J.-S. Photosynthesis genes modulate cadmium tolerance in the freshwater alga *Closterium acutum* revealed by transcriptome analysis. *J. Appl. Phycol.* **2025**, *37*, 1951–1965. [\[CrossRef\]](#)
31. Wang, Y.; Zou, Z.; Su, X.; Wan, F.; Zhou, Y.; Lei, Z.; Yi, L.; Dai, Z.; Li, J. Physiological of biochar and α-Fe₂O₃ nanoparticles as amendments of Cd accumulation and toxicity toward muskmelon grown in pots. *J. Nanobiotechnol.* **2021**, *19*, 442. [\[CrossRef\]](#)
32. Komy, Z.R.; Gabar, R.M.; Shoriet, A.A.; Mohammed, R.M. Characterisation of acidic sites of *Pseudomonas* biomass capable of binding protons and cadmium and removal of cadmium via biosorption. *World J. Microbiol. Biotechnol.* **2006**, *22*, 975–982. [\[CrossRef\]](#)

33. Haider, F.U.; Liqun, C.; Coulter, J.A.; Cheema, S.A.; Wu, J.; Zhang, R.; Wenjun, M.; Farooq, M. Cadmium toxicity in plants: Impacts and remediation strategies. *Ecotoxicol. Environ. Saf.* **2021**, *211*, 111887. [\[CrossRef\]](#) [\[PubMed\]](#)
34. Bouida, L.; Rafatullah, M.; Kerrouche, A.; Qutob, M.; Alosaimi, A.M.; Alorfi, H.S.; Hussein, M.A. A review on cadmium and lead contamination: Sources, fate, mechanism, health effects and remediation methods. *Water* **2022**, *14*, 3432. [\[CrossRef\]](#)
35. Piotrowska-Niczyporuk, A.; Bonda-Ostaszewska, E.; Bajguz, A. Mitigating effect of trans-zeatin on cadmium toxicity in *Desmodium armatus*. *Cells* **2024**, *13*, 686. [\[CrossRef\]](#)
36. Chandrashekharaiyah, P.S.; Sanyal, D.; Dasgupta, S.; Banik, A. Cadmium biosorption and biomass production by two freshwater microalgae *Scenedesmus acutus* and *Chlorella pyrenoidosa*: An integrated approach. *Chemosphere* **2021**, *269*, 128755. [\[CrossRef\]](#)
37. Qi, F.; Gao, Y.; Liu, J.; Yao, X.; Han, K.; Wu, Z.; Wang, Y. Alleviation of cadmium-induced photoinhibition and oxidative stress by melatonin in *Chlamydomonas reinhardtii*. *Environ. Sci. Pollut. Res.* **2023**, *30*, 78423–78437. [\[CrossRef\]](#)
38. Faller, P.; Kienzler, K.; Krieger-Liszkay, A. Mechanism of Cd²⁺ toxicity: Cd²⁺ inhibits photoactivation of Photosystem II by competitive binding to the essential Ca²⁺ site. *Biochim. Biophys. Acta (BBA)—Bioenerg.* **2005**, *1706*, 158–164. [\[CrossRef\]](#)
39. Samadani, M.; Perreault, F.; Oukarroum, A.; Dewez, D. Effect of cadmium accumulation on green algae *Chlamydomonas reinhardtii* and acid-tolerant *Chlamydomonas* CPCC 121. *Chemosphere* **2018**, *191*, 174–182. [\[CrossRef\]](#)
40. Ruan, G.; Liu, C.; Song, G.; Qian, J.; Bao, T.; Zhao, Y.; Sun, S.; Wan, D.; Mi, W.; He, M. Sll1725, an ABC transporter in *Synechocystis* sp. PCC 6803 for the detoxification of cadmium ion stress. *Ecotoxicol. Environ. Saf.* **2025**, *300*, 118389. [\[CrossRef\]](#)
41. Zhang, H.; Heal, K.; Zhu, X.; Tigabu, M.; Xue, Y.; Zhou, C. Tolerance and detoxification mechanisms to cadmium stress by hyperaccumulator *Erigeron annuus* include molecule synthesis in root exudate. *Ecotoxicol. Environ. Saf.* **2021**, *219*, 112359. [\[CrossRef\]](#)
42. Zulfiqar, U.; Jiang, W.; Xiukang, W.; Hussain, S.; Ahmad, M.; Maqsood, M.F.; Ali, N.; Ishfaq, M.; Kaleem, M.; Haider, F.U.; et al. Cadmium Phytotoxicity, Tolerance, and Advanced Remediation Approaches in Agricultural Soils; A Comprehensive Review. *Front. Plant Sci.* **2022**, *13*, 773815. [\[CrossRef\]](#)
43. Xiao, X.; Li, W.; Jin, M.; Zhang, L.; Qin, L.; Geng, W. Responses and tolerance mechanisms of microalgae to heavy metal stress: A review. *Mar. Environ. Res.* **2023**, *183*, 105805. [\[CrossRef\]](#) [\[PubMed\]](#)
44. Zhang, Y.; Li, M.; Chang, F.; Yi, M.; Ge, H.; Fu, J.; Dang, C. The distinct resistance mechanisms of cyanobacteria and green algae to sulfamethoxazole and its implications for environmental risk assessment. *Sci. Total Environ.* **2023**, *854*, 158723. [\[CrossRef\]](#) [\[PubMed\]](#)
45. Elleuch, J.; Hmani, R.; Drira, M.; Michaud, P.; Fendri, I.; Abdelkafi, S. Potential of three local marine microalgae from Tunisian coasts for cadmium, lead and chromium removals. *Sci. Total Environ.* **2021**, *799*, 149464. [\[CrossRef\]](#) [\[PubMed\]](#)
46. Cid, H.A.; Flores, M.I.; Pizarro, J.F.; Castillo, X.A.; Barros, D.E.; Moreno-Piraján, J.C.; Ortiz, C.A. Mechanisms of Cu²⁺ biosorption on *Lessonia nigrescens* dead biomass: Functional groups interactions and morphological characterization. *J. Environ. Chem. Eng.* **2018**, *6*, 2696–2704. [\[CrossRef\]](#)
47. Ozturk, S.; Aslim, B.; Suludere, Z. Cadmium (II) sequestration characteristics by two isolates of *Synechocystis* sp. in terms of exopolysaccharide (EPS) production and monomer composition. *Bioresour. Technol.* **2010**, *101*, 9742–9748. [\[CrossRef\]](#)
48. Tavana, M.; Pahlavan-zadeh, H.; Zarei, M.J. The novel usage of dead biomass of green algae of *Schizomeris leibleinii* for biosorption of copper (II) from aqueous solutions: Equilibrium, kinetics and thermodynamics. *J. Environ. Chem. Eng.* **2020**, *8*, 104272. [\[CrossRef\]](#)
49. Ding, L.; Luo, Y.; Yu, X.; Ouyang, Z.; Liu, P.; Guo, X. Insight into interactions of polystyrene microplastics with different types and compositions of dissolved organic matter. *Sci. Total Environ.* **2022**, *824*, 153883. [\[CrossRef\]](#)
50. Demey, H.; Vincent, T.; Guibal, E. A novel algal-based sorbent for heavy metal removal. *Chem. Eng. J.* **2018**, *332*, 582–595. [\[CrossRef\]](#)
51. Cheng, P.; Chang, T.; Wang, C.; Yao, C.; Zhou, C.; Liu, T.; Wang, G.; Yan, X.; Ruan, R. High cobalt exposure facilitates bioactive exopolysaccharides production with a novel molecular structure in *Botryococcus braunii*. *Chem. Eng. J.* **2022**, *442*, 136294. [\[CrossRef\]](#)
52. Mecozzi, M.; Pietroletti, M.; Tornambè, A. Molecular and structural characteristics in toxic algae cultures of *Ostreopsis ovata* and *Ostreopsis* spp. evidenced by FTIR and FTNIR spectroscopy. *Spectrochim. Acta Part A Mol. Biomol. Spectrosc.* **2011**, *78*, 1572–1580. [\[CrossRef\]](#)
53. Plöhn, M.; Escudero-Onate, C.; Funk, C. Biosorption of Cd (II) by Nordic microalgae: Tolerance, kinetics and equilibrium studies. *Algal Res.* **2021**, *59*, 102471. [\[CrossRef\]](#)
54. Parlanti, E.; Wörz, K.; Geoffroy, L.; Lamotte, M. Dissolved organic matter fluorescence spectroscopy as a tool to estimate biological activity in a coastal zone submitted to anthropogenic inputs. *Org. Geochem.* **2000**, *31*, 1765–1781. [\[CrossRef\]](#)
55. Chen, W.; Westerhoff, P.; Leenheer, J.A.; Booksh, K. Fluorescence excitation–emission matrix regional integration to quantify spectra for dissolved organic matter. *Environ. Sci. Technol.* **2003**, *37*, 5701–5710. [\[CrossRef\]](#) [\[PubMed\]](#)

-
56. Wang, X.; Han, X.; Ge, H. Effect of light intensity on bound EPS characteristics of two *Microcystis* morphospecies: The role of bEPS in the proliferation of *Microcystis*. *J. Oceanol. Limnol.* **2022**, *40*, 1706–1719. [[CrossRef](#)]
 57. Ruan, G.; Mi, W.; Yin, X.; Song, G.; Bi, Y. Molecular Responses Mechanism of *Synechocystis* sp. PCC 6803 to Cadmium Stress. *Water* **2022**, *14*, 32. [[CrossRef](#)]

Disclaimer/Publisher’s Note: The statements, opinions and data contained in all publications are solely those of the individual author(s) and contributor(s) and not of MDPI and/or the editor(s). MDPI and/or the editor(s) disclaim responsibility for any injury to people or property resulting from any ideas, methods, instructions or products referred to in the content.